

# $K^-$ and $\bar{p}$ deeply bound atomic states

E. Friedman and A. Gal

*Racah Institute of Physics, The Hebrew University, Jerusalem 91904, Israel*

## Abstract

The strongly absorptive optical potentials  $V_{\text{opt}}$  which have been deduced from the strong-interaction level shifts and widths in X-ray spectra of  $K^-$  and  $\bar{p}$  atoms produce effective repulsion leading to substantial suppression of the *atomic* wave functions within the nucleus. The width of atomic levels then saturates as function of the strength of  $\text{Im } V_{\text{opt}}$ . We find that ‘deeply bound’ atomic states, which are inaccessible in the atomic cascade process, are generally narrow, due to this mechanism, over the entire periodic table and should be reasonably well resolved. These predictions are insensitive to  $V_{\text{opt}}$ , provided it was fitted to the observed X-ray spectra. In contrast, the *nuclear* states bound by  $V_{\text{opt}}$  are very broad and their spectrum depends sensitively on details of  $V_{\text{opt}}$ . We discuss production reactions for  $K^-$  atomic states using slow  $K^-$  mesons from the decay of the  $\phi(1020)$  vector meson, and the  $(\bar{p}, p)$  reaction for  $\bar{p}$  atomic states. Rough cross-section estimates are given.

*PACS:* 21.65.+f; 36.10.Gv

*Keywords:* Kaonic atoms; Antiprotonic atoms; Deeply bound states;  $(K^-, p)$ ,  $(\phi, K^+)$ ,  $(\bar{p}, p)$  reactions

Corresponding author: E. Friedman,

Tel: +972 2 658 4667, Fax: +972 2 658 6347,

E mail: elifried@vms.huji.ac.il

February 9, 2008

## I. INTRODUCTION

Deeply bound hadronic atom levels have been observed recently for pions [1,2], using the ( $d, {}^3\text{He}$ ) recoilless reaction [3] on  ${}^{208}\text{Pb}$ , following earlier predictions that the  $1s$  and  $2p$  atomic levels in pionic Pb have widths of order 0.5 MeV, significantly less than the approximately 1.5 MeV spacing [4,5]. This striking narrowness is due to the well established repulsive  $s$ -wave part of the pion-nucleus potential at threshold which pushes the corresponding atomic wave functions out of the nucleus such that their overlap with the nucleus, and hence with the imaginary part of the potential, is substantially reduced. A similar, but not as favourable situation might occur for  $\Sigma^-$  atoms due to the inner repulsion of the  $\Sigma$  nucleus potential [6–8]. Such deeply bound hadronic atom levels are inaccessible via the atomic cascade process because of the large absorptive widths compared to the radiation widths. The interest in observing such ‘deeply bound’ atomic levels stems from anticipating a larger overlap of the corresponding wave functions with the nuclear density profile, and hence a greater sensitivity to the hadron-nucleus strong interaction than is the case for normal states.

The other hadronic atom species which have been studied experimentally, consisting of  $K^-$  and  $\bar{p}$  atoms, do not appear at first sight likely candidates for narrow deeply bound states, since the real part of the hadron-nucleus potential at threshold is known for these hadronic species to be strongly attractive and, furthermore, the imaginary (absorptive) part is particularly strong, reaching (absolute) values of order 50 - 100 MeV inside nuclei [9]. However, it was noted years ago by Krell [10] and by Koch et al. [11,12] for  $K^-$  atoms, and by Green et al. [13,14] for  $\bar{p}$  atoms, that the strong absorptive potential for these species made the optical potential at threshold effectively repulsive, even in the presence of a relatively strong attractive real potential, as evidenced by the repulsive atomic level shifts reproduced by the fitted optical potential  $V_{\text{opt}}$ . It was argued in these works that for strong absorptivities the atomic wave functions  $\psi$  are substantially suppressed within the nucleus and that the atomic level widths might saturate as function of  $\text{Im } V_{\text{opt}}$ . However, the latter effect has not been studied systematically and quantitatively for *realistic* situations. In particular, there have been no reliable calculations for the extent of saturation for widths of atomic levels, resulting from the suppression of  $|\psi|^2$  as function of the strength of the absorptive potential.

Wave function damping and subsequent saturation effects due to absorptive potentials are known in elastic scattering. The introduction of absorptivity, in terms of an imaginary part  $W$  of the optical potential  $V_{\text{opt}} = U - iW$ , often induces repulsion into the description of elastic scattering, leading to expulsion of the elastic channel wave function from the nuclear interior. For example, in the eikonal description of nuclear reactions [15], the wave function is exponentially attenuated by the factor

$$|\psi(b, z)|^2 = \exp \left( -\frac{2}{\hbar v} \int_{-\infty}^z W(b, z') dz' \right) \quad (1)$$

where  $v$  is the hadronic projectile velocity and  $\mathbf{r} = (\mathbf{b}, z)$ . A consequence of this attenuation is that the total reaction cross section  $\sigma_R$ , which measures the loss of incident flux into the absorptive channels, saturates as function of the strength of  $W$ , so that

$$\sigma_R = \int \left( 1 - |\psi(b, z \rightarrow \infty)|^2 \right) d^2b \rightarrow \pi R^2 \quad (2)$$

for square-well potentials of radius  $R$ , as  $W$  is made sufficiently strong.

A similar situation must occur also for hadronic atoms where the ‘outer’ atomic levels (analogous to the elastic channel above) are coupled to the ‘inner’ absorptive channels by the nuclear interaction. This coupling is particularly effective in  $K^-$  and in  $\bar{p}$  atoms due to the strong one-nucleon absorption processes  $K^- + N \rightarrow \pi + Y$ ,  $\bar{p} + N \rightarrow$  mesons, respectively. In fact, for a Schrödinger-type equation, the width  $\Gamma$  of the level is given *exactly* (i.e. not perturbatively) by:

$$\frac{\Gamma}{2} = \frac{\int W(r)|\psi(\mathbf{r})|^2 d\mathbf{r}}{\int |\psi(\mathbf{r})|^2 d\mathbf{r}}, \quad (3)$$

which is the straightforward extension of the equality (2) into the bound state regime. Clearly if  $|\psi|^2$  is expelled from the nuclear domain where  $W = -\text{Im } V_{\text{opt}}$  is operative, then the width  $\Gamma$  may also saturate.

In a recent Letter [16] we demonstrated that the width of  $K^-$  *atomic* levels generally saturates, and that consequently  $K^-$  deeply bound atomic states which are inaccessible in the atomic cascade process are by far narrower than a simple extrapolation from the observed states which are accessible in the atomic cascade process would lead to. Here we report on a comprehensive study of this saturation phenomenon for widths in  $K^-$  atoms, and in parallel also for  $\bar{p}$  atoms. We find that deeply bound atomic states are relatively narrow, becoming as little broad as  $\Gamma_{K^-} \sim 1.7$  MeV and  $\Gamma_{\bar{p}} \sim 1.9$  MeV for the  $1s$  state in Pb, and could in many instances be sufficiently well resolved. Our predictions for these states are insensitive to within a few percents to details of  $V_{\text{opt}}$ , provided it was fitted to the observed X-ray spectra. In contrast, the *nuclear* states bound essentially by  $V_{\text{opt}}$  are very broad and their spectrum depends sensitively on details of  $V_{\text{opt}}$ . Lastly, we discuss a few candidate production reactions:  $(K^-, p)$  and  $(\phi, K^+)$  for  $K^-$  deeply bound atomic states, using slow  $K^-$  mesons from the decay of the  $\phi(1020)$  vector meson or from its secondary interactions, and  $(\bar{p}, p)$  for  $\bar{p}$  deeply bound atomic states. We give production cross-section estimates which are new for the  $(K^-, p)$  and  $(\phi, K^+)$  reactions, and which for  $(\bar{p}, p)$  follow the calculations already reported in Refs. [17–19]. The latter reaction was used at LEAR [20] searching, with no success, for deeply bound *nuclear* states.

## II. METHODOLOGY

The interaction of hadrons at threshold with the nucleus is described in this work, as well as in all our past work on hadronic atoms, by the Klein-Gordon (KG) equation of the form:

$$\left[ \nabla^2 - 2\mu(B + V_{\text{opt}} + V_c) + (V_c + B)^2 \right] \psi = 0 \quad (\hbar = c = 1) \quad (4)$$

where  $\mu$  is the hadron-nucleus reduced mass,  $B$  is the complex binding energy and  $V_c$  is the finite-size Coulomb interaction of the hadron with the nucleus, including vacuum-polarization terms. Equation (4) assumes that  $V_{\text{opt}}$  behaves as a Lorentz scalar. If  $V_{\text{opt}}$  is assumed to behave as a Lorentz time-component of a four vector, then additional terms involving  $V_{\text{opt}}$ , of order  $(V_c + \text{Re } B)/\mu$  and  $\Gamma/2\mu$ , arise. We have verified that this neglect is

well justified for atomic states. The use of the KG equation for  $\bar{p}$  atoms is also justified as long as spin effects are negligible and one is interested in  $(2j + 1)$  averaging.

For spherically symmetric potentials, the bound state solutions of the KG equation (4) are of the usual form  $\psi_{nlm}(\mathbf{r}) = (u_{nl}(r)/r)Y_{lm}(\theta, \phi)$ . Since  $V_{\text{opt}}$  is complex, the radial wave functions are also complex and satisfy, for each value of the angular momentum  $l$ , the following generalized orthogonality relationship:

$$\int_0^\infty [1 - (V_c + B_{n,n'})/\mu] u_{n,l}(r) u_{n',l}(r) dr = 0, \quad (n \neq n') \quad (5)$$

where  $B_{n,n'} = (B_n + B_{n'})/2$ . For  $n = n'$ , the normalization integral on the left-hand side remains arbitrary. It could be fixed by replacing the zero on the right-hand side of Eq. (5) by  $\delta_{nn'}$ . We chose not to follow this prescription, but rather kept up with the Schrödinger ‘decaying state’ normalization [21]

$$\int_0^\infty u_{nl}^2(r) dr = 1. \quad (6)$$

Here, two conditions are incorporated: (i) a normalization condition on  $(\text{Re } u)^2 - (\text{Im } u)^2$ , and (ii) the orthogonality of  $\text{Re } u$  and  $\text{Im } u$  which usually is satisfied by  $\text{Im } u$  having one node more than the number of ‘nuclear’ nodes possessed by  $\text{Re } u$ . This enables to classify bound states by the node structure of  $\text{Re } u$  as is outlined below.

Another consequence of the KG equation (4) is the following exact integral expression for the width  $\Gamma = 2 \text{Im } B$ :

$$\frac{\Gamma}{2} = \frac{\int W(r) |\psi(\mathbf{r})|^2 d\mathbf{r}}{\int |\psi(\mathbf{r})|^2 [1 - (\text{Re } B + V_c)/\mu] d\mathbf{r}} \quad , \quad (7)$$

generalizing Eq. (3) due to the presence of the quadratic  $(V_c + B)^2$  term in Eq. (4).

### A. Optical potentials

Several optical potentials were used in order to check the model dependence of the results. In all cases the potentials were obtained from fits to experimental data for normal hadronic atoms. The basic form of the potential is the phenomenological density dependent (DD) potential of Friedman et al. [22,23], given by:

$$2\mu V_{\text{opt}}(r) = -4\pi(1 + \frac{\mu}{m})b(\rho)\rho(r) \quad , \quad (8)$$

$$b(\rho) = b_0 + B_0(\frac{\rho(r)}{\rho_0})^\alpha \quad , \quad (9)$$

where  $b_0$  and  $B_0$  are complex parameters determined from fits to the data,  $m$  is the mass of the nucleon,  $\rho(r)$  is the nucleon-center density distribution normalized to the number of nucleons  $A$  and  $\rho_0 = 0.16 \text{ fm}^{-3}$  is a typical central nuclear density. For  $B_0 = 0$ , the

usual ‘ $t\rho$ ’ potential is obtained. For kaonic atoms we used either a ‘ $t\rho$ ’ potential with the values  $b_0=0.62+i0.92$  fm, or the DD potential with  $b_0=-0.15+i0.62$  fm,  $B_0=1.66-i0.04$  fm,  $\alpha = 0.24$ , with the latter potential providing an improved fit to the data and also respecting the low density limit (c.f. Table 6 of Ref. [9]). It is interesting to note that these potentials are very different from each other in the nuclear interior, e.g. the real attractive potential is about 80 MeV deep for the ‘ $t\rho$ ’ model and 180 MeV deep for the DD model. The nuclear densities used for kaonic atoms were mostly of the ‘macroscopic’ (MAC) type, obtained from phenomenological fits to electron scattering data by unfolding the proton charge distribution. Some calculations were repeated with ‘single particle’ (SP) nuclear densities [9].

For antiprotons two forms of potential were used, a ‘ $t\rho$ ’ form as discussed above or its  $p$ -wave extension given by:

$$2\mu V_{\text{opt}}(r) = q(r) + \nabla \cdot \alpha(r) \nabla \quad (10)$$

with

$$q(r) = -4\pi(1 + \frac{\mu}{m})b_0\rho(r) \quad (11)$$

$$\alpha(r) = 4\pi(1 + \frac{\mu}{m})^{-1}c_0\rho(r). \quad (12)$$

The nuclear densities were always of the SP type, as these lead to better fits [24] to the data, presumably because they provide a more realistic description than the MAC densities at large radii on account of having slopes determined by the least bound nucleons. The parameter values were (c.f. Table 8 of Ref. [9])  $b_0 = 2.5+i3.4$  fm for the  $t\rho$  potential, and  $b_0 = 4.5+i4.5$  fm,  $c_0 = -4.0-i2.4$  fm<sup>3</sup> for the  $p$ -wave extension.

## B. Numerical procedure

Hadronic atoms are physical systems where some unusual features play important role. Whilst effects of the strong interaction are the main topic of studies of such atoms, in most cases the system is dominated by the Coulomb interaction between the hadron and the nucleus. The strong interaction is usually confined (at least for ‘normal’ hadronic atom states) to a small (nuclear) region of the atom but its strength is such that perturbation approach is totally inadequate. The wave function is modified very strongly in the nuclear region, causing long range effects throughout the atom. For this reason care must be exercised in the numerical description of such systems.

The first obvious test is to make sure that the binding energy obtained numerically for the point charge Coulomb interaction agrees with the analytic KG binding energy (except that the test is not possible for  $s$ -states in nuclei with  $Z > 137/2$ ). This is easily fulfilled to an accuracy of 5-7 significant digits. Note that, except for the tests, we always use the Coulomb potential due to the extended nuclear charge distribution and include also the first order vacuum polarization potential.

Another test which is particularly relevant in the present context relates to the width of the level. The width is given by twice the imaginary part of the complex binding energy  $B$  as

obtained from solving numerically the KG equation (4). The width is also given exactly by the integral expression Eq. (7). We routinely get agreement to at least 5 digits between the widths calculated for realistic potentials using the two methods. The approximate expression for the width given by Eq. (3) misses the exact result by 0.2 to 0.5% for atomic states.

Last but not least is the need to ensure that the calculated atomic states are correctly classified. As is discussed later, in the present case of strongly attractive potentials there are *nuclear* bound states in addition to the atomic states, and there are subtle connections between the two kinds of wave functions that greatly affect the latter. In all cases we have also calculated the energies of strongly bound nuclear states whose widths are typically tens of MeV up to over 100 MeV. As such they are insignificant experimentally but their existence affect markedly the atomic states, as the wave functions of the latter satisfy the generalized orthogonality relationship Eq. (5) with the wave functions of the former, for each value of the angular momentum  $l$ . This requirement together with the dependence of the calculated widths on the strength of the imaginary potential help to identify states unambiguously as either deeply bound atomic states or nuclear states.

### III. ENERGY SPECTRA

#### A. Calculations of energy levels

Calculations of energies and widths of kaonic atom levels were made for three representative nuclei over the periodic table: carbon, nickel and lead using different potentials as outlined above. The results for carbon, shown in Ref. [16] will not be repeated here. Figure 1 shows calculated energy levels for Ni for several values of  $l$ . The bars stand for the full width  $\Gamma$  of the level and the centers of the bars correspond to the binding energies  $\text{Re } B$ . The lowest lying level for each value of  $l$  corresponds to a circular orbit with radial number  $n = l + 1$ . The higher levels are for increasing values of  $n$ . The  $4f$  level is the last one populated in the atomic cascade process and its position and width are known experimentally. Similar results for Pb are shown in Fig. 2. In this example the last experimentally observed level is  $7i$ . It is seen that the energy levels are quite well defined also in this example of a heavy nucleus, but it is clear that only with an  $l$ -selective process there is a chance to observe such states experimentally. The dependence on the model is found to be negligibly small; replacing the  $t\rho$  potential by the DD potential or replacing the MAC density by the SP density change the widths by less than 5% and change the binding energies by typically 3% of the width, thus making the calculated spectra essentially model independent, *provided* one employs an optical potential which produces good fits to normal kaonic atom data.

Calculations of binding energies and widths of levels of  $\bar{p}$  atoms were made with the  $t\rho$  potential Eq. (8) and with its  $p$ -wave extension Eq. (10) using SP densities. Figures 3 and 4 show calculated energy level spectra for carbon and zirconium, respectively, elements for which normal  $\bar{p}$  atoms have been observed and the present potentials reproduce the data quite well. Figure 5 shows predictions for Pb, for which no experimental results are available. For this heavy nucleus the levels are quite close to each other although the spectrum is still well defined. Experimental observation of such levels clearly must depend on selectivity in  $l$  values. The dependence of the results on the model is less than for deeply bound kaonic atoms, again provided one uses potentials which fit data for normal states.

## B. Mechanism for narrowing of energy levels

The calculated narrow deeply bound levels in hadronic atoms demonstrated above may seem surprising at first, particularly as they are obtained in the presence of strongly *attractive* real potentials. This phenomenon appears to be quite universal and the mechanism behind it may be understood by studying the dependence of strong interaction level shifts and widths on the hadron-nucleus potential and by examining the wave functions. Figure 6 shows calculated shifts and widths for the  $1s$  level in kaonic Ni as functions of the imaginary part of  $b_0$  when the real part of  $b_0$  is being held at its nominal value, using the  $t\rho$  potential. It is seen that at about 15% of the nominal value of  $\text{Im } b_0$  (of 0.92 fm) the width already saturates and then it goes slowly down, while the shift stays essentially constant at a very large repulsive value. The saturation of widths as function of the imaginary potential is not confined to deeply bound states. Figure 7 shows similar results for the experimentally observed  $4f$  level in Ni. The width saturates at 10% of the nominal value of  $\text{Im } b_0$  but the (very small) shift changes rapidly so that for  $\text{Im } b_0 = 0.92$  fm both shift and width agree with experiment. Figure 8 shows similar behaviour for the  $2p$  level in kaonic Pb. These results may be understood by studying the various wave functions.

Figure 9 shows the absolute value squared of the radial wave function for the  $2p$  state in kaonic Pb for several combinations of potentials. The dashed curve (C) is for the Coulomb interaction only, which is always included. Note that if this wave function is used in the integral Eq. (3) a width of more than 100 MeV is obtained. The solid curve (F) is for the full optical potential added and it shows essentially total expulsion of the wave function from the nucleus (whose rms radius is about 5.5 fm). The dotted curve (Im) is when only the imaginary potential is added, and it shows that the imaginary potential is dominant in determining the wave function. These two curves show that the imaginary potential causes sufficient repulsion such that the overlap between the atomic wave function and the nucleus becomes very small compared to the pure Coulomb case, thus reducing dramatically the width of the level, as is expected from Eq. (3). The dot-dashed curve (Re) shows the wave function when only the real optical potential is added. This *strongly attractive* potential is seen to cause a substantial *repulsion* of the wave function which is a phenomenon peculiar to hadronic atoms. The three small inner peaks preceding the main peak well outside the nucleus indicate that three strongly bound states exist in this real potential, and since the real atomic wave function is approximately orthogonal to the wave functions of these states, it develops nodes, giving rise to the inner peak structure. This structure causes the main *atomic* peak of the wave function to shift to larger radii compared to the Coulomb wave function, thus resulting in a repulsive shift. The repulsion by the attractive real potential is by no means a universal phenomenon. The effect depends on the  $l$ -value of the state and on the positions of the internal nodes of the radial wave function; attractive shifts are also possible although in most cases we have observed repulsion. In the presence of the strong imaginary potential, the internal structure gets suppressed but practically the same node structure remains for  $\text{Re } \psi$ . The node structure inside the nucleus depends critically on the real optical potential and so are the energies of the strongly bound states. Replacing the  $t\rho$  potential for kaonic atoms by the DD potential, the number of nodes changes but the position of the *outermost* node changes very little. The calculated energies of the atomic states hardly change at all.

## IV. PRODUCTION OF DEEPLY BOUND ATOMIC STATES

The deeply bound atomic states discussed in the present work cannot be observed by studying the spectra of X-rays emitted during the atomic cascade process. Direct nuclear reactions, designed to implant strangeness for  $K^-$  atomic states, or antimatter for  $\bar{p}$  atomic states, are necessary in order to produce such states. The lesson gained recently from searching for and discovering deeply bound  $\pi^-$  atomic states [1,2] is that, for a worthy candidate reaction, the hadron has to be produced with as little momentum as possible, in order to maximize the overlap with typical atomic wave functions. Judged from the point of view of momentum transferred from the projectile to the ejectile, this means looking for as low momentum transfer reaction as possible, say,  $q \leq 50$  MeV/c. For pionic atoms the reaction chosen was  $(d, {}^3\text{He})$ , using 600 MeV deuterons and looking for peaks in the energy spectrum of the forward moving  ${}^3\text{He}$  nuclei at energies corresponding to just below the  $\pi^-$  production threshold [3]. Further advantages of such production reactions are that the suppressive effects of the nuclear absorption on the production cross sections are weaker than for other reactions, and that since the momentum transfer is minimal, so is the angular momentum transfer:  $\Delta l \approx 0$ . This latter condition ensures *selectivity*, namely that the atomic states most copiously produced are those for which  $l_h = l_N$ , where  $l_h$  is the orbital angular momentum of the produced atomic hadron and  $l_N$  is that of the target pick-up nucleon. Below, we discuss several suitable reactions for producing  $\bar{p}$  and  $K^-$  deeply bound states.

### A. The forward $(\bar{p}, p)$ reaction

In this reaction an incoming antiproton hits a proton in the target nucleus  ${}^AZ$  and gets captured in  $\bar{p}$  atomic states of the resulting  ${}^{A-1}(Z-1)$  core nucleus, while the proton flies off in the forward direction. Neglecting binding effects, the momentum transfer is zero in the forward direction, corresponding to  $180^\circ$  backward elastic scattering of antiprotons off protons in the c.m. system. The  $(\bar{p}, p)$  reaction was used at the LEAR facility, CERN, at incoming momentum  $p_L = 550$  MeV/c on C, Cu and Bi targets, to search for deeply bound *nuclear* states [20]. The measured energy spectra showed no clear evidence of a peak which could be identified as a  $\bar{p}$  bound state. However, it is far from clear that the protons from this reaction on nuclei are observable at all on top of a large physical background arising from  $\bar{p}$  annihilation, followed by secondary proton emission due to pion absorption. Baltz et al. [19] calculated a ‘signal to background’ ratio  $R \sim 0.01 - 0.04$  in  ${}^{16}\text{O}$  for the leading  $\Delta l = 0$  contribution, which would be very difficult if not impossible to detect experimentally. In this example, the more favorable ratio  $R$  belongs to the  $2p$  *atomic* state, even though its forward excitation cross section is suppressed by 3 orders of magnitude from about 0.5 mb/sr for the most bound and very broad  $\bar{p}$  nuclear  $p$  state to about 0.5  $\mu\text{b/sr}$  for this most bound, but narrow ( $\Gamma \sim 28$  keV)  $\bar{p}$  atomic  $2p$  state. When the relatively large cross section of nuclear states is smeared in accordance with the large width, it yields even poorer signal than for narrow atomic states. However, the ratio  $R$  introduced in that work implicitly assumes perfect energy resolution, whereas the actual resolution  $\Delta E \sim 1$  MeV in the experiment [20] is considerably larger than the natural line width of the  $\bar{p}$  atomic  $p$  states, so the ratio  $R$  would have to be reduced by roughly a factor 30.



Gibbs and Kaufmann [18] observed that in certain favorable cases the  $(\bar{p}, p)$  cross section to atomic states are enhanced due to a coincidence of a relatively sizable radial overlap between the bound proton and antiproton and a large spectroscopic factor for this proton orbit in the target ground state. In particular, they evaluated the transition from the  $2s$  proton state in  $^{31}\text{P}$  to the  $1s$   $\bar{p}$  atomic state in the core nucleus of  $^{30}\text{Si}$  which in their calculation was bound by 1.15 MeV with a width  $\Gamma = 106$  keV. The forward  $(\bar{p}, p)$  cross section, as revised in Ref. [19], is about  $10 \mu\text{b/sr}$ , over an order of magnitude larger than for the example of  $^{16}\text{O}$  target discussed above. Since the  $2p$   $\bar{p}$  atomic state in  $^{30}\text{Si}$  should lie only about 250 keV higher than the  $1s$  atomic state, it is clear that an extremely high resolution ( $\Delta E \sim 100$  keV) is absolutely essential in searching for the few enhanced atomic  $\bar{p}$  states. The forward  $(\bar{p}, p)$  cross section for the production of the  $2p$  atomic state ( $\Delta l = 1$ ) is smaller by about a factor 17 than for producing the  $1s$  atomic state ( $\Delta l = 0$ ) so it may be safely neglected at  $\theta = 0^\circ$ . However, the  $\Delta l = 1$  production cross section of the  $2p$  atomic state peaks at about  $6^\circ$ , where it assumes a comparable value to that of the  $\Delta l = 0$  cross section for the  $1s$  atomic state.

For heavier  $\bar{p}$  atoms, the lowest lying  $1s$  and  $2p$  atomic states lie practically on top of each other, judging from Figs. (4, 5) for the  $\bar{p}$  atomic spectra in Zr and Pb. The  $2p$  atomic state could be explored by doing the  $(\bar{p}, p)$  reaction at the very forward direction on the  $2p_{1/2}$  proton in  $^{89}\text{Y}$  or  $^{90}\text{Zr}$ . A rough estimate of the forward cross section gives  $0.1 \mu\text{b/sr}$ . The  $1s$  atomic state could be explored by doing the  $(\bar{p}, p)$  reaction at the very forward direction on the  $3s_{1/2}$  protons in  $^{208}\text{Pb}$ . The isomeric  $11/2^-$  state of the daughter core nucleus  $^{207}\text{Tl}$  at excitation energy 1.35 MeV could be used to explore the  $\Delta l = 0$  component of the  $(\bar{p}, p)$  reaction in  $^{208}\text{Pb}$ , due to the filled  $h_{11/2}$  proton shell, leading to the  $6h$   $\bar{p}$  atomic state. As seen in Fig. 5, the only states which overlap this state would require  $\Delta l \geq 2$  for their excitation, which might then be neglected at the very forward direction.

## B. Production of $K^-$ atomic states

This subject has not been considered quantitatively, to the best of our knowledge. Hirenzaki et al. [25] very recently proposed to use the  $(K^-, \gamma)$  reaction in order to search for deeply bound  $K^-$  atomic states. We note that the momentum transfer in this reaction is less favorable for this purpose than that of the  $(K^-, p)$  reaction discussed below. For example, for slow  $K^-$  mesons resulting from the decay of  $\phi(1020)$  at rest, the momentum transfer in the  $(K^-, \gamma)$  reaction is about  $q \sim 110$  MeV/c, more than twice as large as for the  $(K^-, p)$  reaction. It is also about twice as large as the momentum transfer, for 20 MeV incident pions, in the  $(\pi^-, \gamma)$  reaction which was tried without much success at TRIUMF [26] to search for deeply bound  $\pi^-$  atomic states. The main difficulty which must be overcome in trying to isolate a low energy photon (or hadron) signal is the considerable low-energy background expected from competing absorption processes.

The  $(K^-, p)$  reaction for producing  $K^-$  atomic states appears conceptually the closest one to  $(\bar{p}, p)$  for  $\bar{p}$  atomic states. Here, an incoming  $K^-$  meson hits a target proton and gets captured in  $K^-$  atomic states of the daughter  $A-1(Z-1)$  core nucleus, while the proton flies off in the forward direction. However, since now the masses are unequal,  $m_K \neq m_N$ , the momentum transfer in the  $(K^-, p)$  reaction differs from zero except at rest. Neglecting binding energy corrections and nuclear recoil, the momentum transfer in the forward direction

is given by:

$$q(0^0) = [T_L (T_L + 2m_N)]^{1/2} - p_L \quad , \quad (13)$$

where  $p_L$  and  $T_L$  are the  $K^-$  incoming momentum and kinetic energy, respectively, in the laboratory (L) frame. For a typical low-momentum  $K^-$  beam at the Brookhaven AGS, with  $p_L = 600$  MeV/c, the momentum transfer given by Eq. (13) is 182 MeV/c, which is too high to be useful. Lowering the incoming momentum further down to  $p_L = 400$  MeV/c, the resulting value  $q(0^0) = 135$  MeV/c still appears too high.

A source of low-energy  $K^-$  mesons is now available at the Frascati  $\Phi$ -Factory  $e^+e^-$  collider DAΦNE due to the decay at rest of the  $\phi(1020)$  meson to  $K^+K^-$  pairs. For the appropriate value of  $p_L = 127$  MeV/c and  $T_L = 16$  MeV, Eq. (13) gives  $q(0^0) = 47$  MeV/c which is sufficiently small to make DAΦNE a possible site for searching for deeply bound  $K^-$  atomic states. Although forward cross sections as large as  $0.1 \mu\text{b/sr}$  may be expected, a major problem in doing this experiment, as mentioned above, would be the need to detect unambiguously the low energy outgoing proton, if one is interested in deeply bound atomic states which are inaccessible to the cascade process. (Otherwise X-rays can be detected from such stopping  $K^-$ ). If the decay at rest of the  $\phi(1020)$  meson were to take place at close proximity to a nucleus such that the kaonic atom recoiled as a whole, then the signature of such a reaction would be a peak in the energy spectrum of the associated  $K^+$  above the end-point of the normal  $K^+$  spectrum. However, the relatively high momentum transfer in this process,  $q = 181$  MeV/c, does not make it a favorable candidate reaction.

Another idea due to members of the GSI collaboration searching for meson-nuclear bound states [27] is to form the  $\phi$  meson in the nucleus using a quasi-free reaction, e.g.

$$\bar{p} + p \rightarrow \pi^0 + \phi \quad , \quad (14)$$

or similarly

$$\bar{p} + n \rightarrow \pi^- + \phi \quad , \quad (15)$$

or even

$$\bar{p} + p \rightarrow \omega^0 + \phi \quad , \quad (16)$$

where the lighter meson in the final state is observed in the forward direction. For  $\bar{p}$  incoming momentum  $p_L = 5.3$  GeV/c, the  $\phi$  meson is produced at rest in the reactions (14,15). The reaction (16) enables the use of lower energy antiprotons, with  $p_L = 1.4$  GeV/c, to get  $\phi$  at rest. The  $\phi$  mesons thus formed decay into  $K^-K^+$  pairs, providing a source of low-energy  $K^-$  ‘beam’ tagged by the observation of  $K^+$  in the opposite direction.

It would be interesting to look for secondary nuclear interactions of the  $\phi$  meson prior to its decay. A suitable reaction in this respect is the recoilless ( $\phi, K^+$ ) reaction:

$$\phi + {}^A_Z \rightarrow K^+ + {}^A_{K^-}Z \quad , \quad (17)$$

where  ${}^A_{K^-}Z$  stands for the kaonic atom made by attaching a  $K^-$  meson to the nuclear target  ${}^A_Z$ . Neglecting nuclear recoil, the momentum transferred in this reaction from the  $\phi$  to the forward  $K^+$  meson is zero provided

$$p_L = m_\phi((m_\phi/2m_K)^2 - 1)^{1/2} = 262 \text{ MeV/c.} \quad (18)$$

To reach this incoming momentum, the reaction (14) could be used at a considerably lower energy than argued above, namely at  $p_L = 0.95 \text{ GeV/c}$ , where the  $\phi$  meson moves backward with a momentum given by (18). As for the reaction (16), it gives *at rest*  $\phi$  mesons of about this momentum. Furthermore, the photoproduction reaction

$$\gamma + p \rightarrow p + \phi \quad (19)$$

also gives  $\phi$  mesons with this backward momentum, for  $p_L = 3.14 \text{ GeV/c}$ .

The  $(\phi, K^+)$  reaction in some respects is analogous to the  $(n, p)$  reaction which was the one proposed originally by Toki and Yamazaki [5] for producing deeply bound  $\pi^-$  atomic states. In both reactions the projectile ( $\phi$  or  $n$ , respectively) decays off shell

$$\phi \rightarrow K^+ + K^- \quad , \quad n \rightarrow p + \pi^- \quad , \quad (20)$$

into the ejectile ( $K^+$  or  $p$ , respectively) plus the negatively charged hadron ( $K^-$  or  $\pi^-$ , respectively) which gets attached to the nuclear target in the atomic state described by a coordinate-space wave function  $\psi_{nlm}(\mathbf{r})$ . The conditional probability to form such an atomic state is given by  $|\tilde{\psi}_{nlm}(\mathbf{q})|^2$ , where  $\tilde{\psi}$  is the Fourier transform of  $\psi$ , and  $\mathbf{q}$  is the momentum transfer in the nuclear reaction. The cross section for the  $(\phi, K^+)$  reaction Eq. (17) may be estimated fairly reliably in the plane-wave approximation (PWA), since the nuclear interactions of both  $\phi$  and  $K^+$  are known to be rather weak. This is not the case for the  $(n, p)$  reaction, however, where the distortion effects on the incident neutron and outgoing proton reduce the PWA cross sections by typically two orders of magnitude [28]. Following Ref. [5], we estimate in the PWA the forward-angle  $(\phi, K^+)$  cross sections for  $q \ll p_L$  by

$$\frac{d\sigma^{\text{PWA}}}{d\Omega} \approx \frac{g_{\phi K \bar{K}}^2}{96\pi^2} \frac{p_L^2}{m_K} \sum_m |\tilde{\psi}_{nlm}(\mathbf{q})|^2 \quad , \quad (21)$$

where only the dominant  $q$  dependence, due to the atomic wave function  $\tilde{\psi}$ , was retained. The coupling constant  $g_{\phi K \bar{K}}$  is determined by the rate of the on-shell  $\phi$  decay into  $K^+ K^-$  pairs. It also satisfies approximately the F-type SU(3) symmetry relationship

$$g_{\phi K \bar{K}}^2 = \frac{1}{2} g_{\rho \pi \pi}^2 \quad (22)$$

where  $g_{\rho \pi \pi} = 6.04$  is determined from the  $\rho^0 \rightarrow \pi^+ \pi^-$  decay.

For the ‘magic’ value of  $p_L$  (Eq. (18)),  $q \approx 2p_L \sin(\theta/2)$ ; Eq. (21) which is valid only at small angles assumes then the form

$$\frac{d\sigma^{\text{PWA}}}{d\Omega} \simeq 0.155 \times (2l+1) |\tilde{R}_{nl}(q)|^2 \quad \text{mb} \quad , \quad (23)$$

where the momentum space radial wave function  $\tilde{R}_{nl}$  (dimension  $\text{fm}^{3/2}$ ) is related to  $R_{nl} = u_{nl}(r)/r$  in coordinate space [c.f. the discussion centered about Eqs. (5,6) in Sec. II] by

$$\tilde{R}_{nl}(q) = \sqrt{4\pi} \, i^l \int_0^\infty j_l(qr) R_{nl}(r) r^2 dr . \quad (24)$$

For small values of  $q$ , the wave functions  $\tilde{R}_{l=0}(q)$  decrease rapidly with  $q$ , whereas the wave functions  $\tilde{R}_{l \neq 0}(q)$  start from zero at  $q = 0$  and reach their respective maxima at finite values  $q = q_{\max}^{(l)}$ ; the larger  $l$  is, the larger  $q_{\max}^{(l)}$  is. Moving gradually away from  $\theta = 0$  ( $q = 0$ ), the  $(\phi, K^+)$  reaction will favor formation of  $K^-$  atomic states with increasingly larger  $l$  values. We have evaluated this momentum space wave function for  $K^-$  atomic  $1s$  states at  $q = 0$  across the periodic table. For the  $1s$  states in Ni and Pb, c.f. Figs. 1 and 2, the values of  $\tilde{R}_{1s}(0)$  are

$$\text{Ni : } 265 - i49.5 \text{ fm}^{3/2} , \quad \text{Pb : } 268 + i116 \text{ fm}^{3/2} , \quad (25)$$

showing little variation as function of  $Z$ . This is a direct consequence of the strong repulsion induced by  $\text{Im } V_{\text{opt}}$  which keeps  $R_{nl}(r)$  apart in spite of the increasingly attractive  $V_c(r)$  as function of  $Z$ . Substituting these values in Eq. (23) we obtain

$$\frac{d\sigma^{\text{PWA}}}{d\Omega}(0^\circ) \simeq 11.3 \text{ b (Ni)} , \quad 13.2 \text{ b (Pb)} . \quad (26)$$

Using distorted waves for the  $\phi$  and  $K^+$  is not expected to reduce these values by more than a factor of 5, judging for example from the distorted wave calculations reported by Dover and Gal [29] for the production of surface  $\Xi$  hypernuclear states in the  $(K^-, K^+)$  reaction. These fantastically large cross sections should not come as a surprise. In this reaction the incoming  $\phi$  meson serves as a very efficient source of  $K^-$  mesons which are then scattered quasi-elastically into well localized *atomic* regions of coordinate space. If one could scatter elastically  $K^-$  mesons off an absorptive object of size  $a \sim 12$  fm (about which the  $1s$   $K^-$  atomic states in Ni and Pb are localized), the *diffractive* forward elastic scattering cross section would be

$$\frac{d\sigma^{\text{el}}}{d\Omega}(0^\circ) \sim \left(\frac{1}{2}p_L a\right)^2 a^2 = 91.4 \text{ b} , \quad (27)$$

for  $p_L = 262$  MeV/c [Eq. (18)]. Note the  $a^4$  dependence on the size parameter  $a$ . Thus, the diffractive  $(\phi, K^+)$  reaction to these  $1s$   $K^-$  atomic states exhausts less than 15% of the bound suggested by the elastic scattering. For realistic situations, however, finite angular resolution will effectively reduce the above diffractive cross sections by 1-2 orders of magnitude.

More quantitative work is needed to embed the  $(\phi, K^+)$  reaction within a full reaction calculation which considers also the propagation and decay of the  $\phi$  meson in the nuclear medium subsequent to its formation.

## V. SUMMARY AND CONCLUSIONS

Calculations of binding energies of  $K^-$  and  $\bar{p}$  atoms based on *realistic* optical potentials, i.e. potentials that lead to good agreement between measured and calculated strong interaction effects in hadronic atoms, revealed rich spectra of well separated energy levels in regions

inaccessible to the common X-rays cascade process. As both types of hadronic atoms are characterised by strongly attractive and absorptive potentials, the results may seem surprising at first sight. The relative narrowness of these deeply bound states is found to result from the effective repulsion due to the strong absorption, which suppresses substantially the overlap between atomic wave functions and the nucleus, thus leading to greatly reduced widths. The effective repulsion is dominated by the imaginary part of the potential, whereas the effects of the real potentials are marginal.

The calculated spectra of deeply bound states show remarkable insensitivity to the details of the potentials, provided one uses potentials that fit hadronic atom data for ‘normal’ states. However, experimental observation of deeply bound states may provide new insight into the interaction of the respective hadrons with nuclei at rest, because the overlap of the atomic wave functions of deeply bound states with nuclei are significantly larger than the overlap for normal states. In order to observe such deeply bound states one must find processes where a  $K^-$  meson or a  $\bar{p}$  are formed with a relatively small (50 MeV/c) momentum transfer in an  $l$ -selective process. Several such examples were given in the preceding section. Particular emphasis was placed on reactions which use low energy  $\phi$  mesons as a doorway to inject  $K^-$  mesons into deeply bound  $K^-$  atomic states.

This research was partially supported by the Israel Science Foundation.

## REFERENCES

- [1] T. Yamazaki et al., Z. Phys. A 355 (1996) 219.
- [2] T. Yamazaki et al., Phys. Lett. B 418 (1998) 246.
- [3] S. Hirenzaki, H. Toki and T. Yamazaki, Phys. Rev. C 44 (1991) 2472.
- [4] E. Friedman and G. Soff, J. Phys. G: Nucl. Phys. 11 (1985) L37.
- [5] H. Toki and T. Yamazaki, Phys. Lett. B 213 (1988) 129.
- [6] C.J. Batty, E. Friedman and A. Gal, Phys. Lett. B 335 (1994) 273.
- [7] C.J. Batty, E. Friedman and A. Gal, Prog. Theor. Phys. Suppl. 117 (1994) 227.
- [8] J. Mareš, E. Friedman, A. Gal and B.K. Jennings, Nucl. Phys. A 594 (1995) 311.
- [9] C.J. Batty, E. Friedman and A. Gal, Phys. Reports 287 (1997) 385; note that in Eq.(11)  $V_c^2$  should read as  $(V_c + B)^2$ , as in Eq. (4) of the present paper.
- [10] M. Krell, Phys. Rev. Lett. 26 (1971) 584.
- [11] J.H. Koch, M.M. Sternheim and J.F. Walker, Phys. Rev. Lett. 26 (1971) 1465.
- [12] J.H. Koch, M.M. Sternheim and J.F. Walker, Phys. Rev. C 5 (1972) 381.
- [13] A.M. Green and S. Wycech, Nucl. Phys. A377 (1982) 441.
- [14] A.M. Green, W. Stepien-Rudzka and S. Wycech, Nucl. Phys. A399 (1983) 307.
- [15] R.J. Glauber, in Lectures in Theoretical Physics, Vol. 1, eds. W.E. Brittin et al. (Interscience, New York, 1959), p. 315.
- [16] E. Friedman and A. Gal, nucl-th/9902036, Phys. Lett. B in press.
- [17] H. Heiselberg, A.S. Jensen, A. Miranda and G.C. Oades, Phys. Lett. 132B (1983) 279.
- [18] W.R. Gibbs and W.B. Kaufmann, Phys. Lett. 145B (1984) 1.
- [19] A.J. Baltz, C.B. Dover, M.E. Sainio, A. Gal and G. Toker, Phys. Rev. C 32 (1985) 1272.
- [20] D. Garreta et al., Phys. Lett. 150B (1985) 95.
- [21] G. Garcia-Calderon and R. Peierls, Nucl. Phys. A265 (1976) 443.
- [22] E. Friedman, A. Gal and C.J. Batty, Phys. Lett. B 308 (1993) 6.
- [23] E. Friedman, A. Gal and C.J. Batty, Nucl. Phys. A 579 (1994) 518.
- [24] C.J. Batty, E. Friedman and A. Gal, Nucl. Phys. A 592 (1995) 487.
- [25] S. Hirenzaki, Y. Okumura, H. Toki, E. Oset and A. Ramos, PANIC 99 Abstracts (Uppsala University, 1999), p.201.
- [26] K.J. Raywood et al., Phys. Rev. C 55 (1997) 2492.
- [27] A. Gillitzer, P. Kienle and T. Yamazaki (private communication).
- [28] J. Nieves and E. Oset, Nucl. Phys. A 518 (1990) 617.
- [29] C.B. Dover and A. Gal, Ann. Phys. [NY] 146 (1983) 309.

# FIGURES

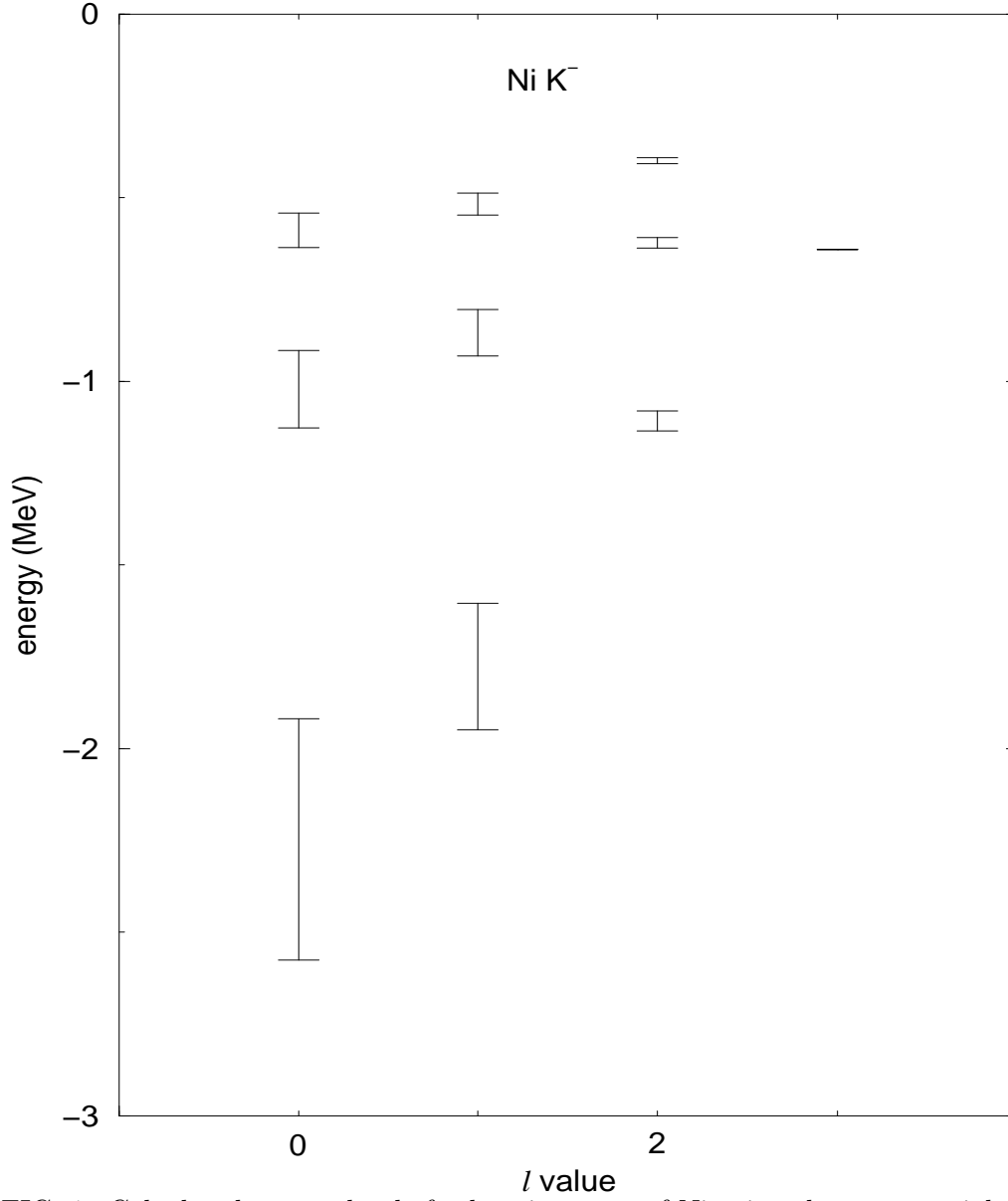


FIG. 1. Calculated energy levels for kaonic atoms of Ni using the  $t\rho$  potential specified in the text. The bars stand for the full width  $\Gamma$  ( $=2 \text{ Im } B$ ) of the levels and the centers of the bars correspond to the energy ( $-\text{Re } B$ ).

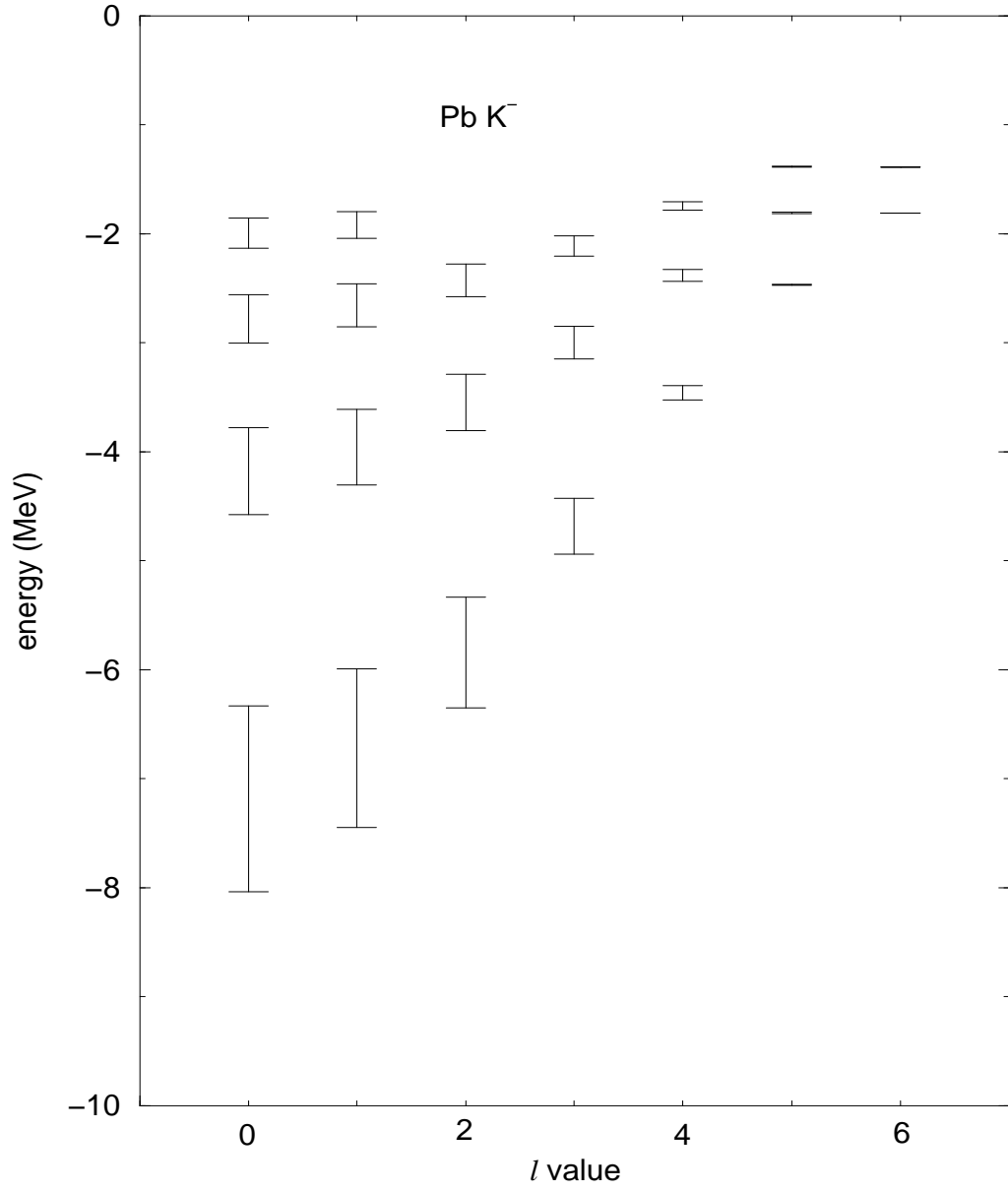


FIG. 2. Calculated energy levels for kaonic atoms of Pb. See caption of FIG. 1 for details.



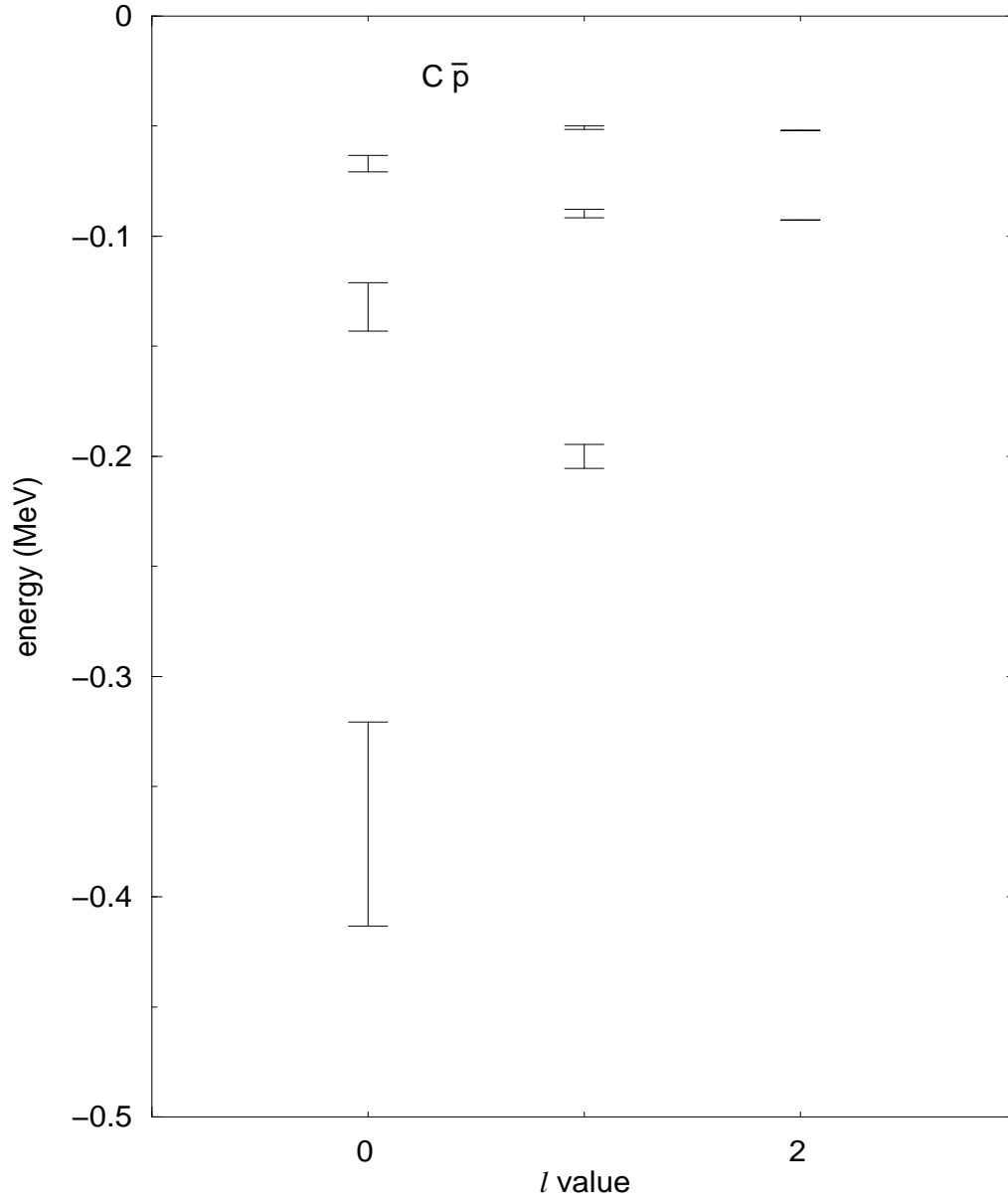


FIG. 3. Calculated energy levels for  $\bar{p}$  atoms of carbon. See caption of FIG. 1 for details.

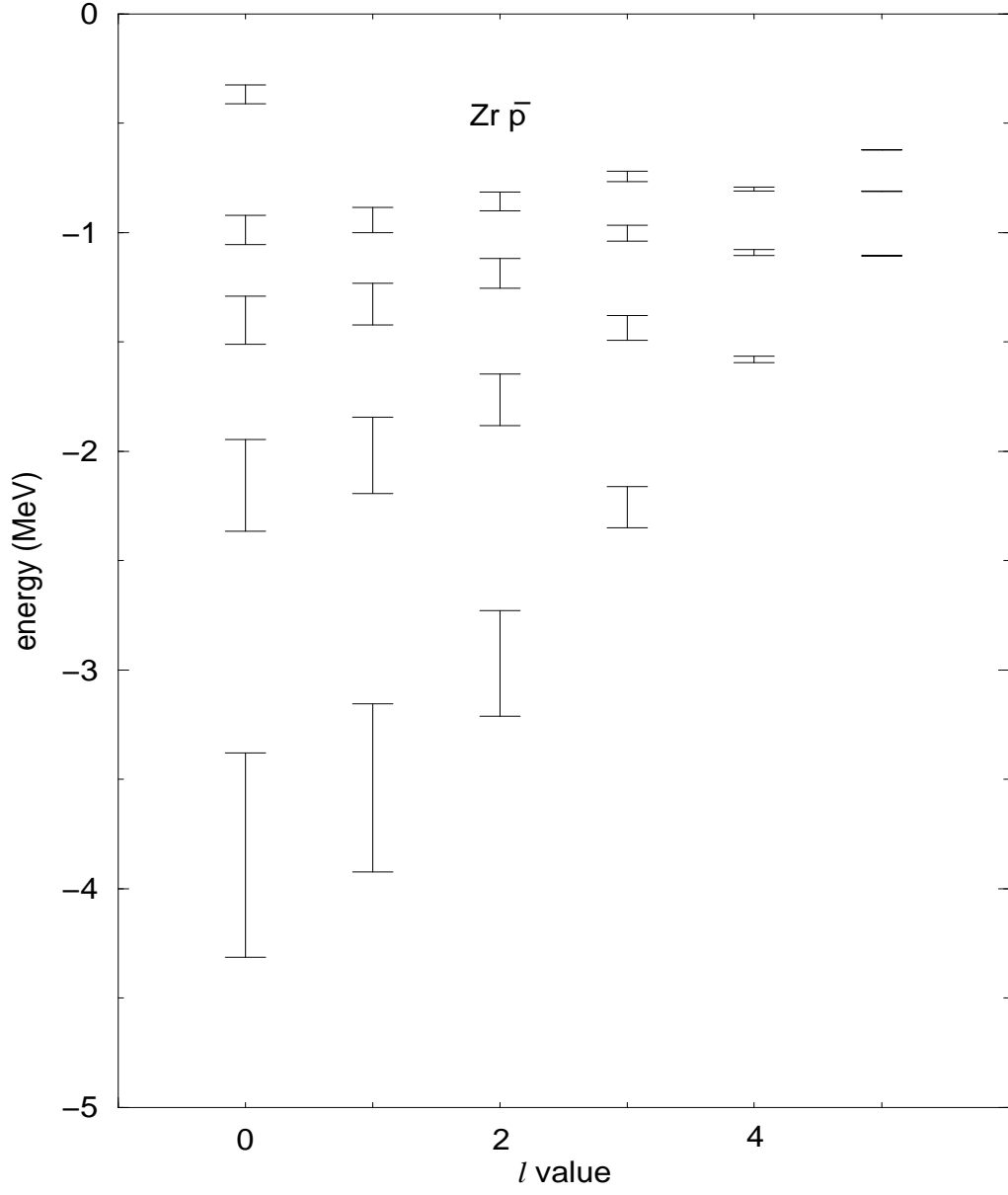


FIG. 4. Calculated energy levels for  $\bar{p}$  atoms of zirconium. See caption of FIG. 1 for details.

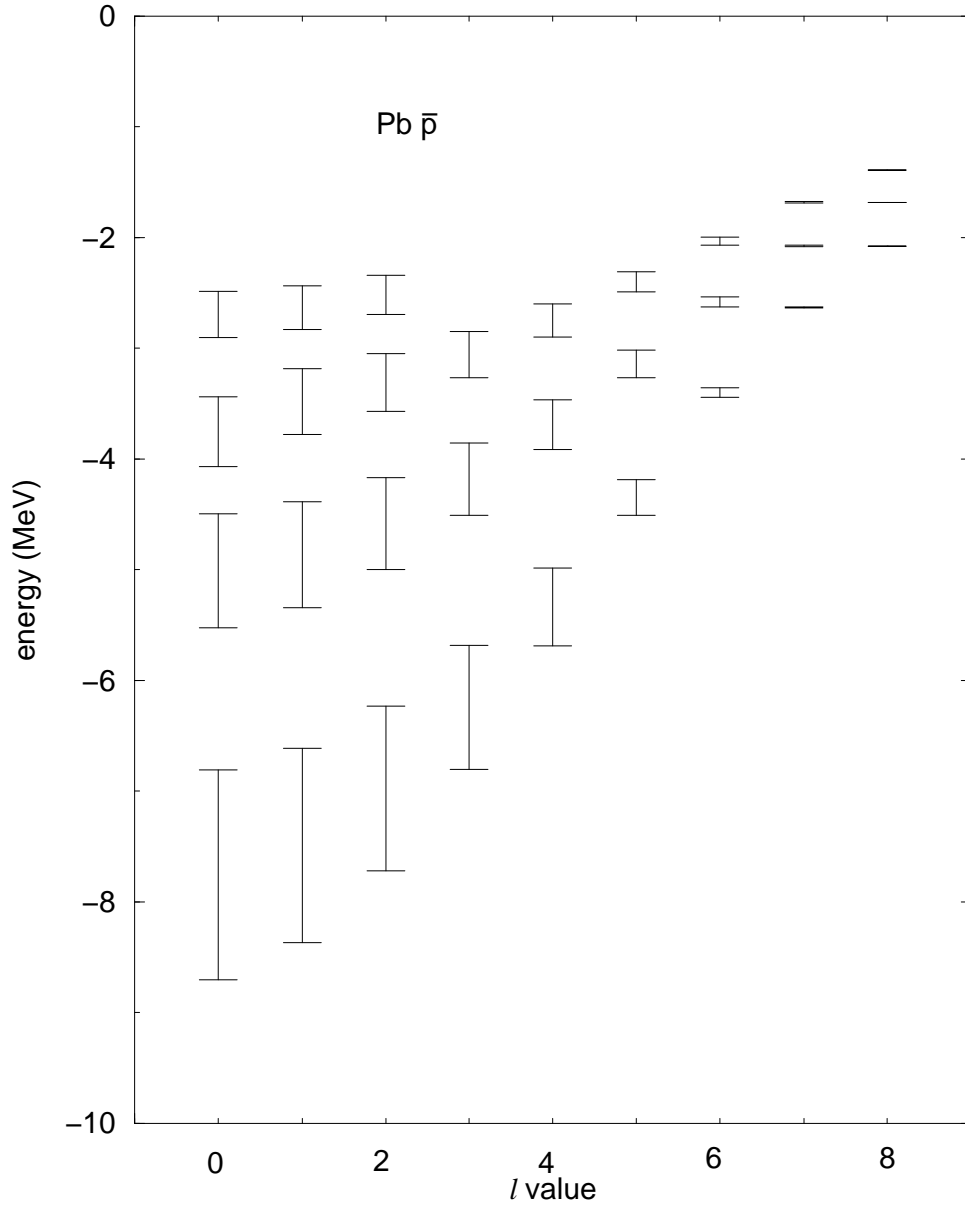


FIG. 5. Calculated energy levels for  $\bar{p}$  atoms of lead. See caption of FIG. 1 for details.

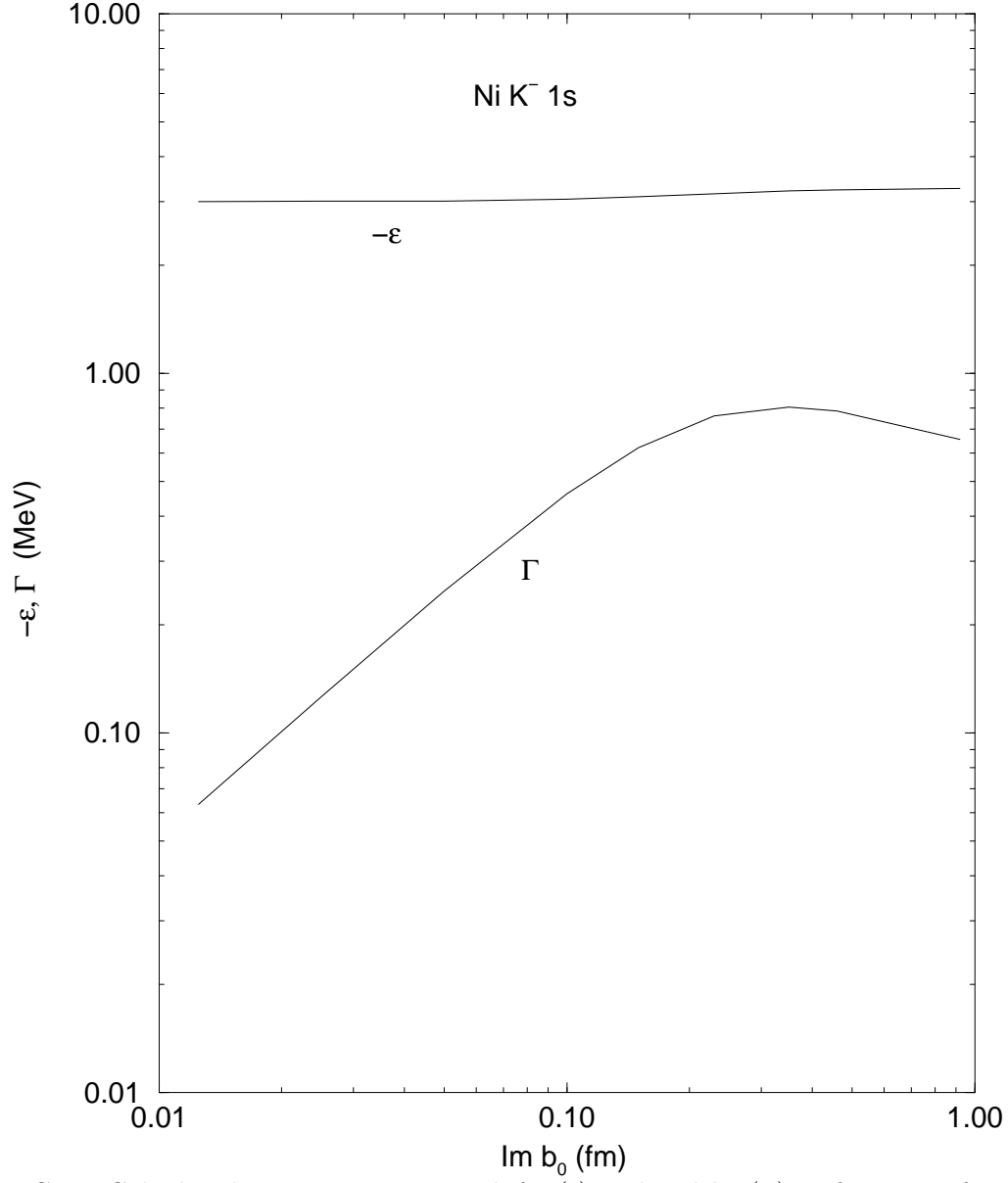


FIG. 6. Calculated strong interaction shifts ( $\epsilon$ ) and widths ( $\Gamma$ ) as function of  $\text{Im } b_0$  for the  $1s$  level in kaonic Ni.  $\text{Re } b_0 = 0.62$  fm.

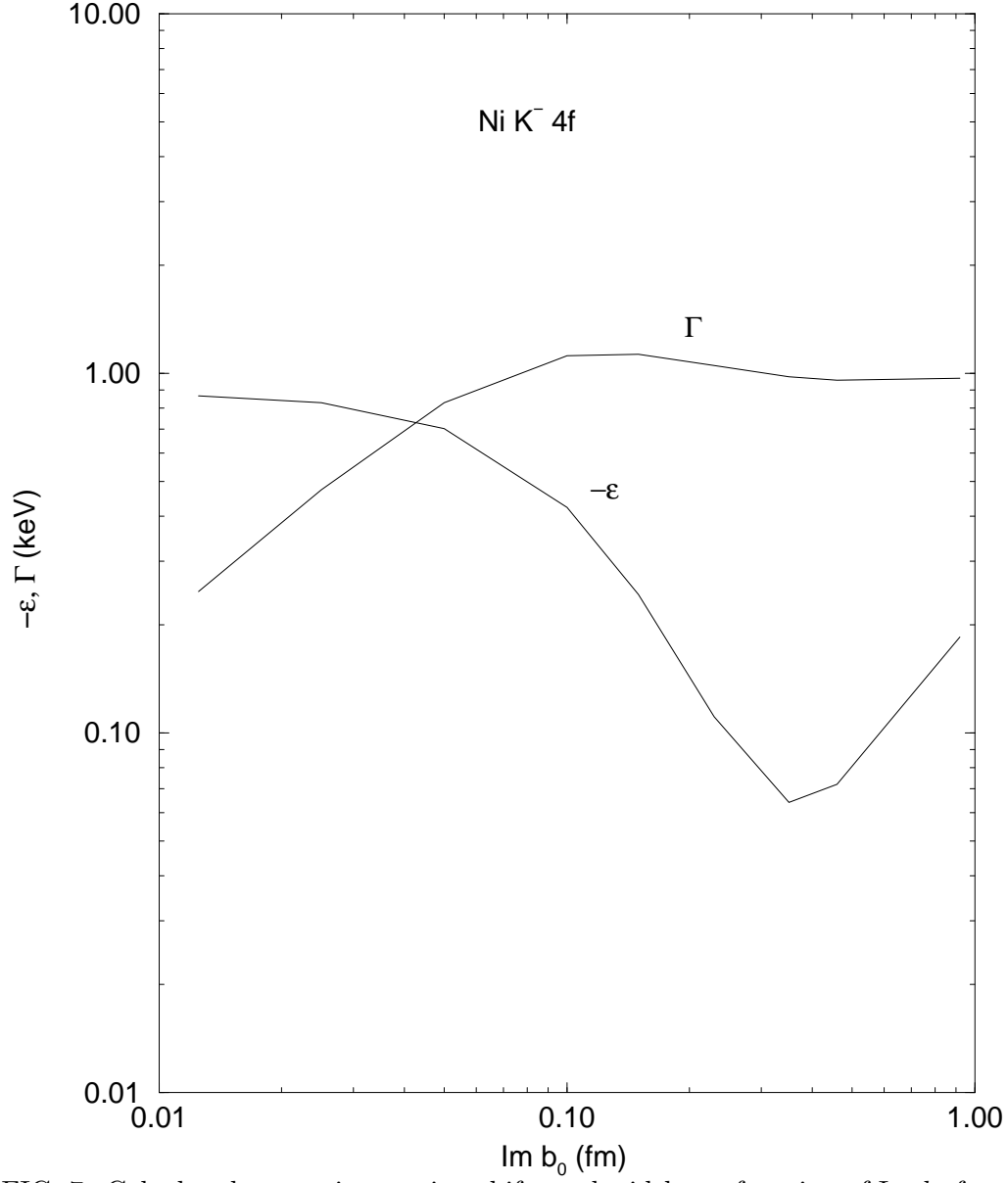


FIG. 7. Calculated strong interaction shifts and widths as function of  $\text{Im } b_0$  for the  $4f$  level in kaonic Ni.  $\text{Re } b_0 = 0.62$  fm.

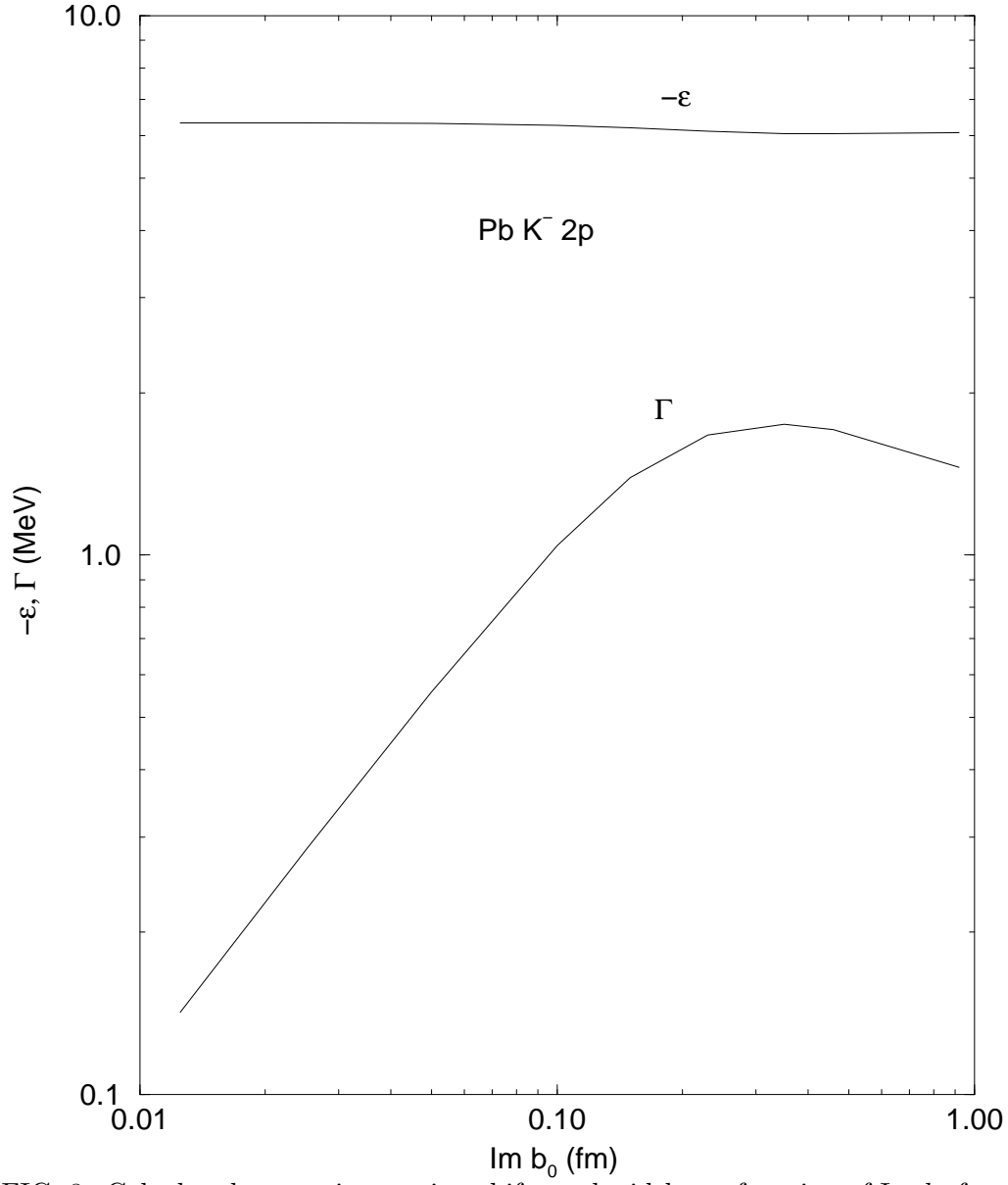


FIG. 8. Calculated strong interaction shifts and widths as function of  $\text{Im } b_0$  for the  $2p$  level in kaonic Pb.  $\text{Re } b_0 = 0.62$  fm.

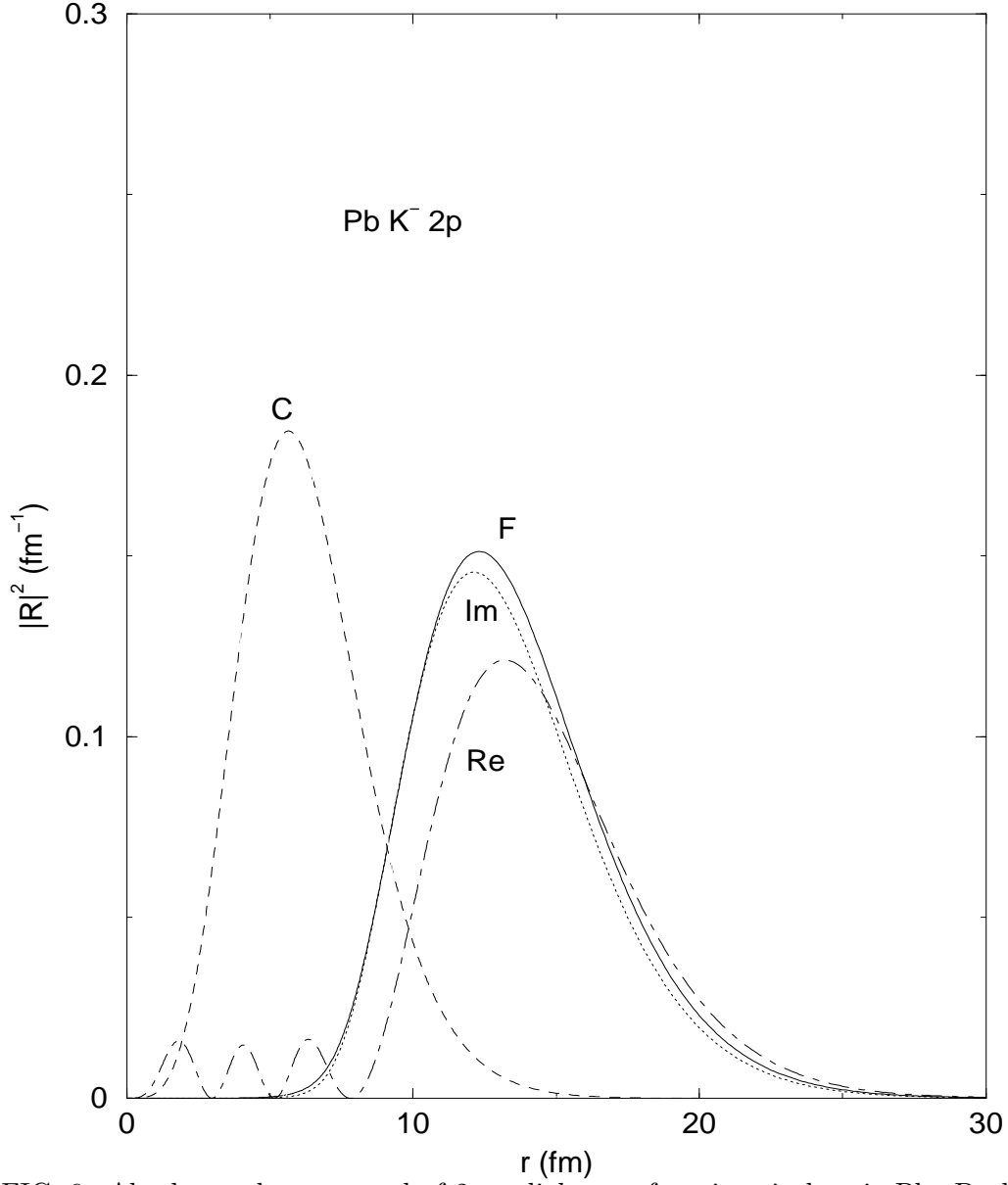


FIG. 9. Absolute values squared of  $2p$  radial wave functions in kaonic Pb. Dashed curve (C) for the Coulomb potential only, solid curve (F) with the full optical potential added, dotted curve (Im) for only the imaginary part of the potential added, dot-dashed curve (Re) for only the real potential added.